

# Time Quasicrystals in Dissipative Dynamical Systems

F. Flicker

Rudolph Peierls Centre for Theoretical Physics, University of Oxford, 1 Keble Road,  
Oxford, OX1 3NP, UK  
Department of Physics, University of California, Berkeley, California 94720 USA  
flicker@physics.org

June 19, 2022

## Abstract

We establish the existence of ‘time quasicrystals’ as stable trajectories in dissipative dynamical systems. These tilings of the time axis, with two unit cells of different durations, can be generated as cuts through a periodic lattice spanned by two orthogonal directions of time. We show that there are precisely two admissible time quasicrystals, which we term the infinite Pell and Clapeyron words, reached by a generalization of the period-doubling cascade. Finite Pell and Clapeyron words of increasing length provide systematic periodic approximations to time quasicrystals which can be verified experimentally. The results apply to all systems featuring the universal sequence of periodic windows. We provide examples of discrete-time maps, and periodically-driven continuous-time dynamical systems.

---

## Contents

<b>1</b>	<b>Introduction</b>	<b>2</b>
<b>2</b>	<b>Quasicrystals</b>	<b>3</b>
<b>3</b>	<b>Symbolic Dynamics</b>	<b>6</b>
3.1	Nonlinear Dynamics Definitions	8
3.2	Symbolic Dynamics Background and Nomenclature	9
3.3	Word Lifting	12
3.4	Maximal Sequences and the Generalized Composition Rule	13
3.5	Application to the Period-Doubling Cascade	14
<b>4</b>	<b>Growing Time Quasicrystals</b>	<b>16</b>
4.1	Admissible Time Quasicrystals	16
4.2	Proof of Maximality of the Pell Words	18
4.3	The Pell Cascade	20
4.4	Other Time Quasicrystals	21
<b>5</b>	<b>Pell Words in Continuous-Time Dynamical Systems</b>	<b>22</b>

5.1	A Continuous-Time Dissipative Autonomous System: the Rössler Attractor	23
5.2	A Continuous-Time Dissipative Driven System: the Forced Brusselator	25
<b>6</b>	<b>Conclusion</b>	<b>28</b>
	<b>References</b>	<b>31</b>

---

## 1 Introduction

The spontaneous breaking of translation symmetry occurs whenever a crystal grows from a liquid. The result is a reduction of the continuous symmetry down to a discrete symmetry, the space group. Recently it was asked whether the same process can occur in time. The name ‘time crystals’ was coined for hypothetical systems which spontaneously break time-translation symmetry in their ground states [1–3]. It later transpired that such a process is impossible [4–6], although a loophole left open the possibility of breaking the *discrete* time translation symmetry of periodically-driven systems down to a multiple of the period [7–10]. This led to a physical implementation in both cold atoms and nitrogen vacancy defects in diamond [11, 12].

Concurrent with these developments, it was realized that the notion of space group symmetry can be extended to include time. These ‘choreographic crystals’ may feature a higher symmetry, when considering their constituent elements in both space and time, than is revealed by any instantaneous snapshot [13]. Additionally, symmetry operations have been identified in periodically-driven ‘Floquet crystals’. Example symmetry operations include so-called time glides, combining a translation in time with a mirror in space [14].

Together these studies establish an understanding of periodicity and disorder on an equal footing in time and space. At first thought these cases seem to exhaust the possibilities for long-range order. Yet there exist long-range ordered objects which are neither periodic nor disordered: between these two extremes we find ‘quasicrystals’, aperiodic tilings consisting of two or more unit cells. Despite lacking periodicity, they nevertheless feature a form of long-range order, which can be seen from the possibility of their construction as slices through higher-dimensional crystals [15–18].

In this paper we demonstrate the existence of *time quasicrystals*: aperiodic tilings of the time axis using unit cells of two different durations. Despite lacking periodicity, they feature long-time order deriving from the fact that the sequence can be generated as a slice through a periodic two-dimensional lattice spanned by two orthogonal directions of time. We identify the time quasicrystals as trajectories within nonlinear dynamical systems, coarse-grained to the scale of simply asking whether we are on the left  $L$  or right  $R$  of the system. The sequence of symbols  $L$  and  $R$  thus obtained matches the sequence of cells of a 1D quasicrystal. We find that precisely two quasicrystal sequences can appear as stable, attracting trajectories in nonlinear systems, which we term the Pell and Clapeyron quasicrystals. We provide a systematic method by which to ‘grow’ these time quasicrystals, showing that each finite-duration periodic approximation is also a stable, attracting trajectory, which provides a method of physically implementing the result. We provide examples from a range of dissipative dynamical systems:

the discrete-time logistic map, the continuous-time autonomous Rössler attractor, and the continuous-time periodically-driven forced Brusselator. Additionally, we present a pedagogical introduction to relevant techniques employed in the field of symbolic dynamics. While well-known in the study of nonlinear systems, these techniques provide a range of possibilities for extending ideas in the fields of time crystals, Floquet crystals, choreographic crystals, and quasicrystals, and it is our hope that in presenting them here further richness of results can be attained in these respective fields.

This paper proceeds as follows. In Sections 2 and 3 we provide background on the subjects of quasicrystals and symbolic dynamics, respectively. The aim is to develop the connections between the areas of study, and so we provide a solid introduction in each case. In Section 4 we present the bulk of our results, demonstrating that, of the ten classes of physically-relevant one-dimensional quasicrystals, precisely two can grow as stable, attracting orbits in discrete-time nonlinear dynamical systems. In Section 5 we extend our results to continuous-time dynamical systems, providing routes to a physically-testable implementation. Finally in Section 6 we provide concluding remarks, and discuss the relationship between time quasicrystals and periodic space-time systems.

## 2 Quasicrystals

Quasicrystals are aperiodic tilings consisting of two or more unit cells. Despite lacking periodicity, the placement of cells is not random: an  $N$ -dimension quasicrystal can be generated as a slice through a  $2N$ -dimensional periodic crystal [15–17]. Certain properties are more naturally expressed in terms of this higher-dimensional crystal. For example, two- or three-dimensional quasicrystals feature discrete rotational symmetries in their diffraction patterns which are forbidden by the crystallographic restriction theorem, which states that only 2-, 3-, 4-, or 6-fold symmetries are allowed for periodic tilings in these dimensions. The symmetries demonstrated by quasicrystals' diffraction patterns (5-fold, 8-fold, 10-fold, and 12-fold [19]) are nevertheless permitted to crystals in the higher-dimensional space through which they were sliced [20–22]. Equivalently we can say that quasicrystals are objects whose reciprocal-space dimension does not match their real-space dimension [16, 17]. A large number of quasicrystals has been grown artificially, and there have even been found two naturally-occurring examples, both in the same Siberian meteorite [23, 24].

We consider the case of one-dimensional quasicrystals, which can be generated by taking a cut through a two-dimensional lattice. Some authors prefer to define quasicrystals in terms of the forbidden rotational symmetries of their diffraction patterns; as rotations are not well-defined in 1D, they instead use the phrase ‘quasilattices’ to refer to these cases. We avoid this distinction in order to emphasize the connection to time crystals, Floquet crystals, and choreographic crystals.

We define a 1D quasicrystal to be an aperiodic tiling of a one-dimensional space with tiles of two different lengths, generated as a cut through a two-dimensional lattice. A necessary but not sufficient condition for an aperiodic tiling of two tiles to be a quasicrystal is that each cell appears with precisely two spacings [25]. In Figure 1 we demonstrate the ‘cut-and-project’ quasicrystal construction: we draw an irrationally-sloped line through the two-dimensional lattice, intersecting a vertex. For simplicity we take a square lattice with a unit cell length of one, but any regular lattice is acceptable. Drawing a second line parallel to the first which



cut-and-project or intersection, using a line whose gradient is the golden ratio  $\varphi$ :

$$\varphi = (\varphi - 1)^{-1} = \frac{1}{2} (1 + \sqrt{5}).$$

Consider again the case where the line intersects a vertex of the lattice. Such cases form a set of zero measure, but are instructive here [25]. From the first intersection of a lattice line after the (unique) intersection with a lattice vertex, the sequence of cells begins as follows:

$$RLR^2LRLR^2LR^2L\dots$$

This is shown in Fig. 1.

The Fibonacci quasicrystal can also be generated by so-called ‘inflation rules’:

$$R \rightarrow RL, \quad L \rightarrow R \tag{1}$$

which are applied to every symbol, starting from the left of the word, at every iteration:

$$\begin{aligned} R &\rightarrow RL \rightarrow RLR \\ &\rightarrow RLR^2L \\ &\rightarrow RLR^2LRLR \\ &\rightarrow RLR^2LRLR^2LR^2L \\ &\rightarrow RLR^2LRLR^2LR^2LRLR^2LRLR \\ &\rightarrow \dots \end{aligned}$$

The lengths of these sequences are the Fibonacci numbers  $F_n$ , and hence they are known as Fibonacci words. The infinite Fibonacci word  $F_\infty$  is the Fibonacci quasicrystal [26].

Note that, while each iteration of the inflation rules leads to extra cells growing on the right of the previous word, the growth mechanism is inherently nonlocal, requiring a substitution of every letter in the word simultaneously. The consistency of the leftmost string of each word is given by a discrete scale invariance implied by the inflation rules: considering the infinite Fibonacci word, while it can be described by the unit cells  $R$  and  $L$ , it can equally-well be described by any inflation of these cells, for example  $RL$  and  $R$ ,  $RLR$  and  $RL$ , *etc.* This property is shared with crystals, which can be described by any integer multiple of their primitive unit cell.

While all quasicrystals can be generated by cut-and-project, only some can be generated by inflation rules [17]. Conversely, inflation rules can generate objects which are not quasicrystals, as we see in Section 3.5 when considering the period-doubling cascade. We can describe the Fibonacci inflation rules by a matrix

$$A = \begin{pmatrix} 1 & 1 \\ 1 & 0 \end{pmatrix}$$

such that

$$A \begin{pmatrix} R \\ L \end{pmatrix} = \begin{pmatrix} R+L \\ R \end{pmatrix}$$

and the  $n^{\text{th}}$  term can be made by instead acting on the vector with  $A^n$ . The eigenvalues of  $A$  are  $\varphi$  and  $\varphi^{-1}$ . In general, quasicrystals of two cell types can be described by matrices such

as this, featuring non-negative integer entries, whose eigenvalues are Pisot-Vijayanarayanan numbers: quadratic irrationals  $a + \sqrt{b}$  with rational  $a, b$ , such that  $a + \sqrt{b} > 1$  and  $0 < |a - \sqrt{b}| < 1$  [17, 25].

There are an infinite number of quasicrystals which can be generated by the intersection method of Figure 1. They fall into equivalence classes. For example, shifting the intersecting line perpendicular to itself generates ‘locally isomorphic’ quasicrystals, where any finite sequence of cells appearing in one appears in the others [15]. Loosely, these can be thought of as translations of one another. Others may be equivalent up to inflations, deflations, or translations of others [25]. While all  $N$ -dimensional quasicrystals can be created through a cut-and-project from a  $2N$ -dimensional lattice, only a subset of these can also be generated through inflation rules [16, 17].

The recent work of reference [25] identifies that, in fact, only ten equivalence classes of 1D quasicrystal exist which are truly physically relevant, in the sense that they relate to higher-dimensional counterparts through their identifying irrational numbers, which describe both the relative lengths of the cell types (volume, in general dimensions), and the relative frequency of the cells’ appearances. In Table 1 we reproduce these quasicrystals and their inflation rules from reference [25]. The physical significance of the ten classes is that their counterparts in two and three dimensions are precisely the quasicrystals which have been grown in the lab, or discovered as naturally-occurring materials [21, 22, 25]. This suggests their suitability for study with an eye to physical implementation. A theoretical argument due to Levitov underpins the experimental observation that all known two- and three-dimensional quasicrystals feature 5- 8- 10- or 12-fold symmetry [19]. The same argument explains why physical quasicrystals relate only to quadratic irrational numbers, whereas a more general class of similar objects can be constructed mathematically [18].

By way of example, consider again the Fibonacci quasicrystal. This has cell lengths related by the golden ratio  $\varphi$ . The length of Fibonacci word  $n$  is the  $n^{\text{th}}$  Fibonacci number  $F_n$ , and we refer to the corresponding word with the same symbol  $F_n$ . The ratio of lengths of successive Fibonacci words also tends to the golden ratio:

$$\varphi = \lim_{n \rightarrow \infty} \frac{F_n}{F_{n-1}}.$$

The Fibonacci quasicrystal generalizes to the two-dimensional case of the Penrose tiling, shown in Figure 2. The Penrose tiling’s diffraction pattern has ten-fold rotational symmetry, forbidden in two-dimensional crystals but allowed in four or five-dimensional crystals through which it can be considered a slice [15, 25]. The ratio of the two cells’ areas, as well as their relative frequency of occurrence, is given by the golden ratio. The full significance of the relationship between the Fibonacci quasicrystal and the Penrose tiling requires a consideration of Coxeter groups and Ammann decorations, explained in detail in references [25, 27].

### 3 Symbolic Dynamics

In this section we present a brief overview of relevant results in the field of symbolic dynamics. Aside from being necessary background to the subsequent sections, the hope is that a pedagogical introduction to the ideas will be useful to authors working in the fields of time crystals, Floquet crystals, choreographic crystals, and quasicrystals. In Section 3.1 we define some

Case	$A$	eigenvalues	slope	$\rho$	$\lambda$
1	$\begin{pmatrix} 1 & 1 \\ 1 & 0 \end{pmatrix}$	$\frac{1}{2}(1 \pm \sqrt{5})$	$\frac{1}{2}(1 \pm \sqrt{5})$	$RL$	$R$
2a	$\begin{pmatrix} 1 & 1 \\ 2 & 1 \end{pmatrix}$	$1 \pm \sqrt{2}$	$\pm\sqrt{2}$	$RL$	$R^2L$
2b	$\begin{pmatrix} 0 & 1 \\ 1 & 2 \end{pmatrix}$	"	$1 \pm \sqrt{2}$	$L$	$RL^2$
3a	$\begin{pmatrix} 1 & 2 \\ 1 & 3 \end{pmatrix}$	$2 \pm \sqrt{3}$	$\frac{1}{2}(1 \pm \sqrt{3})$	$RL^2$	$RL^3$
3b	$\begin{pmatrix} 2 & 1 \\ 3 & 2 \end{pmatrix}$	"	$\pm\sqrt{3}$	$R^2L$	$R^3L^2$
3c	$\begin{pmatrix} 1 & 1 \\ 2 & 3 \end{pmatrix}$	"	$1 \pm \sqrt{3}$	$RL$	$R^2L^3$
4a	$\begin{pmatrix} 3 & 1 \\ 4 & 1 \end{pmatrix}$	$2 \pm \sqrt{5}$	$-1 \pm \sqrt{5}$	$R^3L$	$R^4L$
4b	$\begin{pmatrix} 2 & 1 \\ 5 & 2 \end{pmatrix}$	"	$\pm\sqrt{5}$	$R^2L$	$R^5L^2$
4c	$\begin{pmatrix} 1 & 1 \\ 4 & 3 \end{pmatrix}$	"	$1 \pm \sqrt{5}$	$RL$	$R^4L^3$
4d	$\begin{pmatrix} 0 & 1 \\ 1 & 4 \end{pmatrix}$	"	$2 \pm \sqrt{5}$	$L$	$RL^4$

Table 1: (After [25]). The ten equivalence classes of physically-relevant 1D quasicrystals. The substitution matrix  $A$ , applied to the vector  $(R, L)^T$ , generates the substitutions  $R \rightarrow \rho, L \rightarrow \lambda$  under addition. The ‘slope’ column indicates the slope of the line drawn through a square two-dimensional lattice to generate each sequence by either cut-and-project or intersection. The columns  $\rho$  and  $\lambda$  show the cell sequences generated from  $R$  and  $L$  respectively. Ref [25] identifies a canonical ordering of substituted cells; we do not follow this, as it grows the quasicrystals symmetrically to the left and right of the starting point, whereas we will wish to refer to the right of the generated string as the future. See also the discussion in Section 4.1.

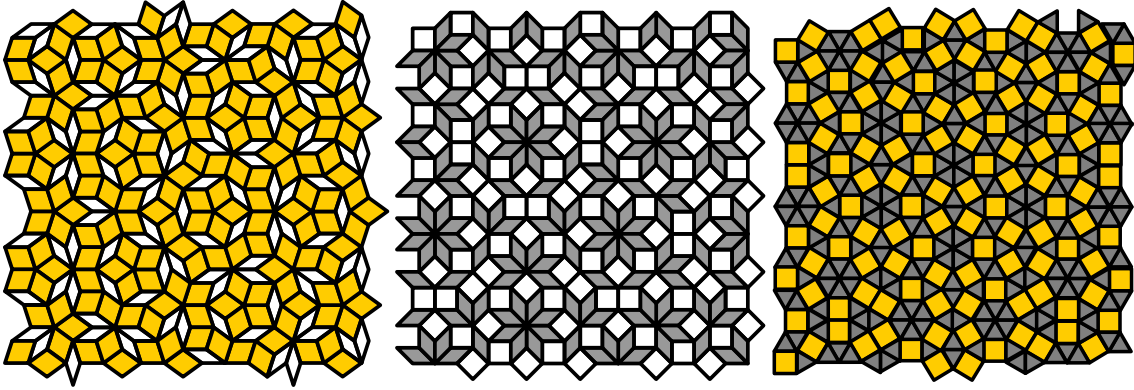


Figure 2: Sections of two-dimensional quasicrystals, after [18]. **Left:** the Penrose tiling. The ratio of the areas of the tiles is the golden ratio  $\varphi$ , as is the relative frequency of occurrence of the two tiles [28]. Approximate 5- or 10-fold symmetry can be seen at different points, and the diffraction pattern features true 10-fold symmetry. This is the two-dimensional generalization of the Fibonacci quasicrystal, which also features cell lengths and relative frequencies in the golden ratio. **Middle:** the Ammann-Beenker tiling. The ratio of cell areas is  $\sqrt{2}$ . The tiles' relative frequencies lie in the silver ratio  $1 + \sqrt{2}$ . Approximate 8-fold symmetry can be seen at points, and the diffraction pattern is 8-fold symmetric [20]. This is the two-dimensional generalization of the Pell quasicrystal, similarly related to the silver ratio. **Right:** The two-dimensional generalization of the Clapeyron quasicrystal (which has cell lengths related by  $2 + \sqrt{3}$ ). The diffraction pattern is 12-fold symmetric.

basic terms in the study of general nonlinear dynamical systems. In Section 3.2 we present the basic ideas of symbolic dynamics. One technique, word lifting, is particularly important to the present work, and Section 3.3 is devoted to it. Section 3.4 presents the ‘generalized composition rule’, which is the key mathematical tool used to prove the existence of time quasicrystals. The results are returned to frequently in later sections. Finally, in Section 3.5, we apply the ideas to the period-doubling cascade into chaos, both as an already well-understood example, and to provide a point of reference when explaining the generalization to the Pell and Clapeyron cascades in Section 4.

### 3.1 Nonlinear Dynamics Definitions

In this section we briefly define some concepts in the study of nonlinear dynamical systems and chaos which will be referred to later in the paper. Detailed introductions and more precise definitions can be found for example in references [26, 29, 30].

Dynamical systems are defined by their equations of motion, which take the general form

$$\dot{\mathbf{x}} = \mathbf{f}(\mathbf{x})$$

with  $\mathbf{x}$  a vector describing the state at a given time. In this paper we will consider  $\mathbf{x}$  to be positions. If the equations are such that they can be rewritten as a Lagrangian

$$L(\mathbf{x}, \dot{\mathbf{x}}) = \frac{1}{2} \dot{\mathbf{x}}^2 - V(\mathbf{x})$$



the system has an associated Hamiltonian and conserves energy; otherwise it is dissipative. If time only enters the equations implicitly via  $\mathbf{x}(t)$  the equations are said to be autonomous, and if time appears explicitly through some driving they are non-autonomous (driven). Non-autonomous equations can be rewritten in an autonomous form by introducing extra variables, as we will show in Section 5 when dealing with the forced Brusselator.

The continuous-time systems we consider in Section 5 feature ‘attractors’, regions which attract trajectories from within a wider ‘basin of attraction’ and to which trajectories converge at infinite time. A ‘strange attractor’ additionally has a fractal structure. A convenient tool for analyzing continuous-time dynamical systems is the Poincaré section, a slice through trajectories. This can be used to construct the Poincaré first-return map, which plots intersection  $n + 1$  of a trajectory with the Poincaré section against intersection  $n$ , provided the trajectory passes through the section in the same direction.

We refer to trajectories in discrete-time maps as ‘orbits’, which need not be periodic (closed). When considering continuous-time systems we will always have in mind the relation to the discrete-time maps via the Poincaré first-return map, and so refer to orbits in these cases also. An orbit is ‘Lyapunov stable’ if all trajectories which start sufficiently close to it remain so for all time [29]. If a Lyapunov-stable orbit is also attracting, then it is said to be stable, although we often reiterate the attracting nature of stable orbits here. The Lyapunov stability of an orbit can be characterized by its Lyapunov exponents, which are calculated using a local linearization of the nonlinear map at a point in time. At a maximum the linear term vanishes. In the cases considered here this leads to ‘superstability’, which can be thought of either as a Lyapunov exponent of  $-\infty$  or as trajectories converging onto the orbit at a faster-than-exponential rate [31]. There is a separate notion of ‘structural stability’, meaning the orbits under consideration are unaffected by sufficiently small changes to the system parameters. All cases considered in this paper are structurally stable.

### 3.2 Symbolic Dynamics Background and Nomenclature

In this section we present a pedagogical introduction to some basic concepts in symbolic dynamics. The ideas are presented clearly in reference [31], an excellent resource. Other classic references include [26, 32–34].

In the majority of this paper we focus on the logistic map:

$$x_{n+1} = 1 - \mu x_n^2 \tag{2}$$

with real-valued  $x \in [-1, 1]$ . Note that this is not the standard writing of the map, but leads to a neater analysis in what follows. The map is shown in Fig. 3 for several choices of the parameter  $\mu$ , along with the corresponding stable, attracting orbits of the dynamics. The logistic map models a discrete-time dissipative dynamical system, with each iteration constituting a time step. Despite the map’s simplicity, it features stable periodic orbits of all periods, as well as chaos [29, 32, 34]. The map was originally introduced as a simplified model of animal population dynamics [35]. Additionally, it falls into the same universality class as a wide range of continuous-time nonlinear dynamical systems. In Section 5 we demonstrate that the results found for the logistic map can be extended to continuous-time dynamical systems of both the autonomous (Rössler) and periodically-driven (forced Brusselator) type. These extensions provide testable predictions for physical systems, but the simplicity of the logistic map makes it invaluable in introducing and proving the relevant ideas.

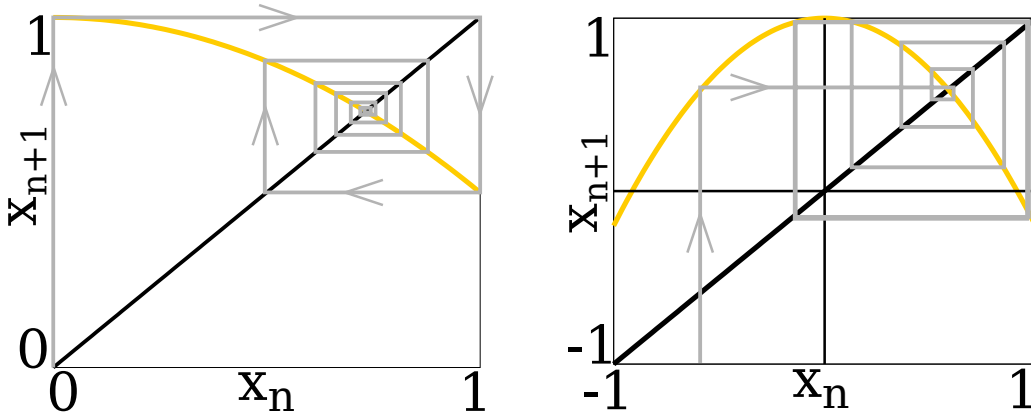


Figure 3: The logistic map  $x_{n+1} = 1 - \mu x_n^2$ . **Left:** for  $\mu = 0.5$  the map features a single stable fixed point. This can be found by the ‘cobwebbing’ technique: draw a vertical line to the map, then a horizontal line to the diagonal  $x_{n+1} = x_n$ , then iterate. This feeds the output of one iteration into the input of the next, and so on. **Right:** for  $\mu = 1.2$  the fixed point is unstable, but there exists a stable period-2 orbit onto which trajectories converge (again found through cobwebbing).

Symbolic dynamics applied to the logistic map entails a coarse-graining to simply asking whether we are on the left,  $L$  ( $x < 0$ ), or right,  $R$  ( $x > 0$ ), of the maximum [32–34]. The  $x_n$  in the iterations are found to an appropriate precision, and recorded. Once the desired number of iterations has been carried out, we assign a letter to each according to whether it is greater or smaller than zero. The central point  $x = 0$  has a special significance, since its appearance in an orbit implies superstability: there is no linear expansion of the curve at its maximum, so the Lyapunov exponent is  $-\infty$ , and trajectories converge faster than exponentially onto such orbits. We denote this point  $C$ . Iterations of the map can be carried out by the ‘cobwebbing’ technique: drawing successive vertical lines to the map and horizontal lines to the diagonal line  $f(x) = x$ . If we consider the set of points of the diagonal line which are hit, and which side of the map they fall onto, we will find a sequence of letters taken from the set  $\{R, L, C\}$ . This sequence of letters is termed a word. When the word is periodic we write only the repeating part. We will be interested in finding ‘admissible’ words: those which describe stable, attracting, orbits.

The superstable period two sequence is described by the word  $RCRC \dots = (RC)^\infty$ , from now on denoted  $RC$ . The word  $LC$  is inadmissible, as there is no intersection of the line  $f(x) = x$  in the range  $-1 < x < 0$ . The admissible words of the logistic map turn out to be universal, in the sense that the same words are the admissible words of any differentiable 1D maps. If the map is additionally unimodal, having a single maximum like the logistic map, the sequence in which the words develop as the parameter  $\mu$  is increased is also universal [33]. It is called the ‘universal sequence’, and it provides a re-ordering of the set of integers (so that each integer appears once as the length of a stable orbit) [36]. Continuous-time dynamical systems fall into this same universality class provided they are sufficiently dissipative. Note that all sufficiently dissipative continuous-time strange attractors have differentiable 1D discrete maps as their Poincaré sections, and all differentiable 1D discrete-time maps can be related to continuous-time attractors [37]. In fact, dissipation may be too strong a requirement, as we discuss in Section 6 when considering non-dissipative Hamiltonian systems.

All orbits longer than two are described by words beginning  $RL$ , as the trajectory first goes to the largest  $x$  it will ever hit (positive, so  $R$ ), then the smallest  $x$  it will hit (negative, so  $L$ ). This provides a useful constraint when searching for quasicrystals, as it specifies that the first cell generated by the inflation rule must be labeled  $R$ , and the second  $L$ . Simple algorithms exist for determining the admissibility of a given word, and therefore dynamical trajectories. Reference [31] gives an extensive explanation of various methods. One of these, the generalized composition rule, we explain and employ shortly.

Despite a great deal of overlap between the study of quasiperiodic dynamical systems and the study of quasicrystals, the latter have not previously been identified as admissible trajectories in dynamical systems. A comment is necessary regarding the relation to quasiperiodic systems, which feature two or more incommensurate frequencies, and which are well-studied in the context of dynamical systems. Quasiperiodic systems could either be described as having an uncountably-infinite number of unit cells of different lengths, or as having one unit cell of infinite length, or neither. Quasicrystals, on the other hand, have a finite number of unit cells, with most studies focussing on the case of two [38]. They therefore feature a minimum and maximum spacing between cells [16, 17]. If we consider an irrationally-sloped line drawn through a 2D lattice, as in Fig. 1, the spacing of intersections of the line with the lattice is quasiperiodic, and may be infinitesimally small. The sequence of symbols generated, however, is a quasicrystal.

References [26, 39] consider a simple linear quasiperiodic system defined by the map

$$x_{n+1} = x_n + \alpha \tag{3}$$

on the interval  $x \in [0, 1)$  (with  $x = 0$  and  $x = 1$  identified) for quadratic irrational  $\alpha$ . By dividing the domain into two partitions, a coarse-graining is defined which leads the quasiperiodic motion to spell the corresponding quasicrystalline word. The lack of nonlinearity, however, makes these states ‘marginally stable’, meaning they have zero Lyapunov exponent, and can be destroyed with infinitesimal perturbations. This is the key difference with the quasicrystalline states we identify here, which maintain their sequences under such perturbations. Stability is key in the present study, as in the previous work on time crystals [7–10].

It should be noted that, in any chaotic regime, all periodic and aperiodic orbits appear but are unstable [34]. This includes both the quasicrystal trajectories we seek, and their periodic approximations. In Anosov chaotic systems, obeying Smale’s Axiom A, unstable orbits have both stable and unstable manifolds [40, 41]. If a trajectory starts on an orbit’s stable manifold, it stays close to the orbit for all time, although it is unstable to perturbations taking it off the manifold. ‘Control of chaos’ involves protocols to direct trajectories onto given stable manifolds, and to stabilize chosen orbits within chaotic systems [42–45]. These techniques require the evolution to be monitored, and tailored perturbations to be added based on both the particular system and the evolution of the trajectory. In the present work we seek to drive a dynamical system *purely periodically*, and to receive a response which spontaneously breaks the symmetry down to that of a quasicrystal. In this way the work generalizes the results of previous work on time crystals, in which a periodic driving received a response breaking the symmetry to a periodic response of twice the period. For this reason we disallow symmetry-breaking perturbations on top of the driving. After the present work appeared online, other work appeared in which a quasicrystalline driving was predicted to generate a quasicrystalline response in time crystals [46]. As we demonstrate that dynamical systems can stabilize a quasicrystalline response from a periodic driving, this effect is also unrelated to ours.

### 3.3 Word Lifting

Once a sequence is established to be admissible, it is necessary to identify the parameter settings which will allow its realization. In the logistic map of Eq (2), it is necessary to identify the parameter  $\mu$ . This process is known as ‘word lifting’ [31].

The logistic map is many-to-one, so its inverse is multivalued. In taking the inverse we have to specify which of the two branches to take, left or right. So define two inverse functions like so:

$$\begin{aligned} f_L^{-1}(x) &\triangleq L(x) = -\mu^{-\frac{1}{2}}\sqrt{1-x} \\ f_R^{-1}(x) &\triangleq R(x) = \mu^{-\frac{1}{2}}\sqrt{1-x} \end{aligned}$$

where ‘ $\triangleq$ ’ indicates a definition. A period- $N$  orbit is defined by

$$f \circ f \circ f \circ \dots \circ f(x) = x$$

with  $N$  nested functions. We will focus on superstable fixed points, which feature the points  $x = 0$  and  $f(0) = 1$ . To invert the sequence of maps we have to specify which branch to take at each iteration. Take the example of the superstable period five sequence  $RLRRC$ :

$$\begin{aligned} f(f(f(f(f(0)))))) &= 0 \\ &\downarrow f(0) = 1 \\ f(f(f(f(1)))) &= 0 \\ &\downarrow \\ f(f(f(1))) &= R(0) \end{aligned}$$

and, inverting the other functions to form the original word,

$$\begin{aligned} 1 &= R \circ L \circ R \circ R(0) \\ 1 &= \mu^{-\frac{1}{2}} \sqrt{1 + \mu^{-\frac{1}{2}} \sqrt{1 - \mu^{-\frac{1}{2}} \sqrt{1 - \mu^{-\frac{1}{2}} \sqrt{1 - 0}}}} \\ &\downarrow \times \mu \\ \mu_{n+1} &= \sqrt{\mu_n + \sqrt{\mu_n - \sqrt{\mu_n - \sqrt{\mu_n}}}} \end{aligned}$$

The indices introduced in the final expression indicate an iterative expression with which to find  $\mu$  numerically. In general, for the logistic map, each letter in the word simply dictates the corresponding  $\pm$  in the sequence in the final expression. As  $\mu$  must still be found numerically, it is simpler to define separate functions for  $R$  and  $L$ , and iterate the expression

$$\mu_n = R_{\mu_{n-1}} \circ L_{\mu_{n-1}} \circ R_{\mu_{n-1}} \circ R_{\mu_{n-1}}(0)$$

where ‘ $\circ$ ’ indicates function composition. It is a testament to the power of the technique that, despite each nested function introducing an additional square root, we are able to apply word lifting to seventy-letter words without issue.

### 3.4 Maximal Sequences and the Generalized Composition Rule

In this section we define some terms and operations used later in the paper. We stick to common conventions, and refer the reader to the references for further explanation and proofs [29, 31, 36].

**Parity of Words:** the parity of a word  $\Sigma$ ,  $P(\Sigma)$ , can be established by the following facts:

$$\begin{aligned} P(R) &= 1 \\ P(L) &= -1 \\ P(\Lambda\Sigma) &= -P(\Lambda)P(\Sigma) \end{aligned}$$

that is, the parity of the word counts the number of  $R$ s; a word with an odd number of  $R$ s is said to be odd, and, somewhat counter-intuitively, has parity  $+1$ .

**Order of Words:** letters are ordered  $L < C < R$ , which just corresponds to their ordering along the real line. Given two words

$$\begin{aligned} W_1 &= W^* \sigma \dots \\ W_2 &= W^* \tau \dots \end{aligned}$$

where  $W^*$  is common to both words, the order of the words is as follows:

$$\begin{aligned} W^* \text{ even, } & \begin{cases} \sigma > \tau & \rightarrow W_1 > W_2 \\ \sigma < \tau & \rightarrow W_1 < W_2 \end{cases} \\ W^* \text{ odd, } & \begin{cases} \sigma > \tau & \rightarrow W_1 < W_2 \\ \sigma < \tau & \rightarrow W_1 > W_2. \end{cases} \end{aligned}$$

Note that the order of two words matches the order in which they appear as  $\mu$  is increased in the logistic map, or the equivalent of  $\mu$  is increased in a general unimodal differentiable map [33, 36].

**Maximal Words:** the significance of maximality is that any superstable periodic orbit is described by a maximal word, and if any maximal word has its last letter substituted with a  $C$  its orbit becomes superstable [34]. A word  $\Sigma$  is maximal iff

$$\Sigma \geq S^k(\Sigma) \quad \forall k$$

where the shift operator  $S^k$  removes the first  $k$  letters of the word (shifts the symbols by  $k$  to the left). If the word is of finite length, it is maximal if it is larger than all its subshifts [26].

**The generalized composition rule:** this is a method of generating maximal sequences by substituting letters into already known maximal sequences. Using the notation that  $\Sigma|_C$  is the word  $\Sigma$  with its final letter substituted with a  $C$ , given a maximal word  $\Sigma$ , the substitutions  $R \rightarrow \rho$  and  $L \rightarrow \lambda$  also yield a maximal word if the following are true:

1.  $P(\lambda) = P(L)$ ,  $P(\rho) = P(R)$
2.  $\rho > \lambda$
3.  $\rho|_C$  is maximal

- 4.  $\rho\lambda|_C$  is maximal
- 5.  $\rho\lambda^\infty$  is maximal.

We again refer to the references for the proof, but note that the first rule ensures that substitutions maintain the parity of the word, and the other rules ensure the substitution's maximality [31].

**The Periodic Window Theorem:** any parameter  $\mu$  corresponding to a superstable orbit must be contained in a window of values  $\mu$  of finite measure corresponding to stable (but not superstable) orbits [31,34]. This can be seen for the logistic map in Fig. 4. Note that while the window is guaranteed to exist and be of finite measure, its actual width is system-dependent, and cannot necessarily be simply determined. It is not even true, for example, that either longer words or later words in the universal sequence have smaller windows [31].

### 3.5 Application to the Period-Doubling Cascade

In order to demonstrate the use of these concepts, we consider the the period-doubling cascade route to chaos in the logistic map. The working in this section is well-understood, but it provides a useful reference when considering the Pell cascade in subsequent sections [29,31,34,47,48]. Period doubling can be generated by repeated use of the substitutions

$$\begin{aligned} R &\rightarrow \rho = RL \\ L &\rightarrow \lambda = RR. \end{aligned} \tag{4}$$

This is the simplest possible nontrivial substitution compatible with the generalized composition rule, as parity (number of  $R$ s) must be preserved, meaning  $\rho$  must have an odd number, and  $\lambda$  an even number, of  $R$ s. Applied to the initial symbol  $R$  we have:

$$\begin{aligned} R &\rightarrow RL \\ &\rightarrow RLR^2 \\ &\rightarrow RLR^3LRL \\ &\rightarrow RLR^3LRLRLR^3LR^3 \\ &\rightarrow RLR^3LRLRLR^3LR^3LR^3LRLRLR^3LRLRL \\ &\rightarrow \dots \end{aligned}$$

The length of the word after  $n$  iterations is  $2^n$ . Figure 4 shows the points cycled between once transients have died down, *i.e.* the points constituting the stable orbit, for each value of  $\mu$  in the logistic map of Eq. (2). The plot is known as an orbit diagram [29]. Inspecting the letters of each word generated by Eq. (4), we find the sequences of points visited in the uppermost part of each periodic window (after the line crosses  $x = 0$ ) in each period doubling in Fig. 4. Since the mapping in Eq. 4 obeys the criteria of the generalized composition rule, and since the starting term  $R$  is maximal and admissible, each term is therefore maximal and admissible.

Some of the smaller periodic cycles are shown to the right of the diagram. For  $\mu < \frac{3}{4}$  there is a single stable fixed point which is converged to for all starting conditions. While the value  $x_\infty$  converged to depends on  $\mu$ , it always lies on the right of the map, so is described by the word  $R$ . At  $\mu = \frac{3}{4}$  there is a period-doubling bifurcation to a stable 2-cycle (period 2

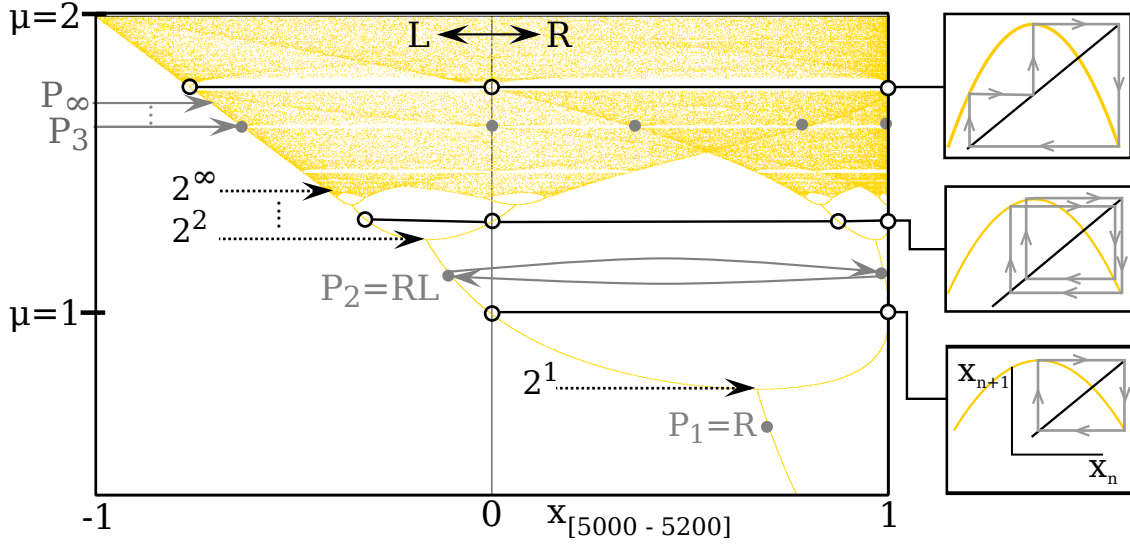


Figure 4: The orbit diagram of the logistic map of equation (2). The map is iterated for 5000 steps at each value of  $\mu$ , to allow stable orbits to converge, then 200 points are plotted. Points  $x < 0$  are on the left of the map, and are labeled  $L$  (labels  $x = 0 : C$ ,  $x > 0 : R$ ). Period doublings are marked with dashed lines. Chaos results above  $2^\infty$  at  $\mu \approx 1.4012$ . The boxes on the right show the superstable orbits of period 2, 4, and 3 (bottom to top). Additionally, the grey solid arrows indicate the sequence of superstable orbits constituting the Pell cascade (Section 4.3). The Pell quasicrystal  $P_\infty$  is reached by  $\mu \approx 1.6703$ .

orbit) which can be found analytically. At  $\mu = \frac{5}{4}$  this period 2 orbit becomes superstable, as it contains the point  $x = 0$  (implying the other point,  $x = 1$ ). This process then repeats an infinite number of times: with increasing  $\mu$ , a stable  $2^n$  orbit described by the word  $\Sigma R$  ( $\Sigma L$ ) becomes superstable,  $\Sigma C$ , then stable  $\Sigma L$  ( $\Sigma R$ ), then a period-doubling bifurcation occurs to orbit length  $2^{n+1}$  (note that the terminal letter alternates, hence the importance of the words' parities). An infinite number of such bifurcations then occurs in a period-doubling cascade, until at around  $\mu \approx 1.42$  period  $2^\infty$  is reached, and a chaotic regime is entered.

The periodic window theorem can be seen in action in Figure 4. The value  $\mu = 1$  corresponds to a superstable period-2 orbit, since  $f(x) = 1 - x^2$  iterates between  $x = 0, 1$ . Symbolically, the corresponding word is  $RC$ . There is a finite range of values  $\frac{3}{4} < \mu < 1$  where the period-2 orbit  $RR$  is stable ( $R$  in our conventions), and a finite range  $1 < \mu < \frac{5}{4}$  where the period-2 orbit  $RL$  is stable. Equivalent results can be seen for the higher period-doubled orbits in the cascade.

It is interesting to note that the period-doubling cascade generated by the substitution rules of Eq. (4) shares many properties with the growth of a quasicrystal: each new word contains the previous word as its leftmost string, and the final word in the period-doubling cascade will consist of an infinitely-long aperiodic string of two symbols with two spacings between each symbol (zero or one between  $R$ s, one or three between  $L$ s) [26]. These are necessary but not sufficient conditions for quasicrystallinity. To check whether the infinitely period-doubled word is a quasicrystal, we can examine its substitution matrix:

$$A = \begin{pmatrix} 1 & 1 \\ 2 & 0 \end{pmatrix}$$

which has eigenvalues 2 and -1. The requirement for a  $2 \times 2$  substitution matrix to define a quasicrystal is that its eigenvalues are Pisot-Vijayanarayanan numbers: one must be greater than one, and the absolute magnitude of the other must be strictly less than one [16, 25]. The period-doubling sequence therefore fails on the grounds that the smaller eigenvalue has a magnitude of *exactly* one. This is why it does not appear in Table 1. While only an infinitesimal difference, it is the difference between rationality and irrationality. There can be no cut-and-project construction corresponding to the matrix  $A$ , since the intersection line would require rational slope 2, which implies a periodic sequence of cells, yet the inflation rules are generating an aperiodic sequence.

## 4 Growing Time Quasicrystals

In this section we present our main results. Building on the background in the previous sections, we demonstrate the existence of ‘time quasicrystals’: tilings of the time axis by two unit cells of different duration, in an aperiodic pattern which can be described as a slice through a two-dimensional tiling of a space spanned by two orthogonal time directions. We require time quasicrystals to be both stable to perturbations, and to attract nearby trajectories in the phase space. We also require them to ‘grow’ in a systematic manner, by inflation rules.

We will show that the quasicrystal cells, labeled  $R$  and  $L$ , correspond to the letters in admissible words in symbolic dynamics, and therefore the points visited at each iteration of a discrete-time differentiable unimodal map coarse-grained into two halves. We consider the specific example of the logistic map, but the results apply to the map’s entire universality class, which contains all discrete-time differentiable 1D maps, as well as continuous-time dynamical systems which are sufficiently dissipative that their dynamics are well-represented by Poincaré sections which are approximately 1D. This point is returned to in Section 5 in which we consider physical implementations of the results.

This section proceeds as follows. In Section 4.1 we identify that there are precisely two physically-relevant 1D quasicrystals admissible as stable attracting orbits in nonlinear dynamical systems. We term these the infinite Pell word, and the infinite Clapeyron word. In Section 4.2 we prove the result rigorously using the tools of symbolic dynamics. Focussing on the simpler Pell word, in Section 4.3 we identify an analogue to the period-doubling cascade route to chaos, which we term the ‘Pell cascade’, which provides a systematic growth mechanism of the infinite Pell word by successive periodic approximations (finite Pell words). These provide a practical method of implementing time quasicrystals in finite-duration experiments.

### 4.1 Admissible Time Quasicrystals

Employing the tools explained in the background sections, proving the existence of time quasicrystals reduces to the task of identifying quasicrystal inflation rules of the form

$$R \rightarrow \rho \quad L \rightarrow \lambda$$

which obey the generalized composition criteria of Section 3.4.

Checking the ten sets of inflation rules listed in Table 1 against the criteria of Section 3.4, it seems that there is only one match. The Fibonacci words of class 1 are ruled out, for example, as the corresponding inflation rules do not preserve the words’ parities. The first



admissible class is 2a, generated by the substitution rules

$$R \rightarrow \rho = RL, \quad L \rightarrow \lambda = RRL. \quad (5)$$

The corresponding substitution matrix

$$A = \begin{pmatrix} 1 & 1 \\ 2 & 1 \end{pmatrix}$$

has eigenvalues  $1 \pm \sqrt{2}$ : the silver ratio and its Galois conjugate. The sequence of words generated by the substitutions applied to  $R$  is

$$\begin{aligned} R &\rightarrow RL \\ &\rightarrow RLR^2L \\ &\rightarrow RLR^2LRLRLR^2L \\ &\rightarrow RLR^2LRLRLR^2LRLR^2LRLR^2LRLRLR^2L \\ &\rightarrow \dots \end{aligned}$$

of lengths 1, 2, 5, 12, 29, 70, ... (sequence A000129 in OEIS [49]). These are known as the Pell numbers,  $P_n$ , after Euler's inaccurate attribution of their discovery to John Pell [50]. We refer to the words as 'Pell words', and denote both the Pell word and its length by  $P_n$ . The silver ratio is to the Pell words  $P_n$  as the golden ratio is to the Fibonacci words  $F_n$ , *i.e.*

$$1 + \sqrt{2} = \lim_{n \rightarrow \infty} \frac{P_n}{P_{n-1}}.$$

The infinite Pell word  $P_\infty$  we term the Pell quasicrystal. This quasicrystal was previously considered in reference [51].

Inspecting the inflation rules of the remaining nine quasicrystal classes other than the Pell quasicrystal, it appears at first that all others are incompatible with the generalized composition rules. However, some care has to be taken, since the inflation rules listed in Table 1 are ambivalent to the labels attached to each cell. For example, class 3a is listed as having substitution rules

$$R \rightarrow RL^2, \quad L \rightarrow RL^3$$

which do not preserve parity (number of  $R$ s). If we relabel the cells  $R \leftrightarrow L$  we have

$$L \rightarrow LR^2, \quad R \rightarrow LR^3$$

which do preserve parity. Additionally, we are free to cyclically permute the letters in the substituted sequences  $\rho$  and  $\lambda$ , as this just corresponds to translating the corresponding quasicrystal by a finite number of symbols (time steps). Cyclic permutation is allowed provided that it preserves the topology of the quasicrystal. This can be understood by attempting to re-order the Pell inflation rules as follows:

$$R \rightarrow RL, \quad L \rightarrow LRR$$

which would lead to the words:

$$R \rightarrow RL \rightarrow RL^2R^2 \rightarrow RL^2R^2LR^3LRL \rightarrow \dots$$

The sequence is not growing a quasicrystal, as it does not obey the necessary condition of having two cell types with two spacings between each cell. On the other hand, the topology-preserving re-ordering

$$R \rightarrow RL, \quad L \rightarrow RLR$$

leads to the words

$$\begin{aligned} R &\rightarrow RL \\ &\rightarrow RLRLR \\ &\rightarrow RLRLR^2LRLR^2L \\ &\rightarrow RLRLR^2LRLR^2LRLRLR^2LRLR^2LRLRLR \rightarrow \dots \end{aligned}$$

which obey the necessary condition, and can be seen to be leading to a translation of the usual Pell quasicrystal (simply note that the distribution of  $R$ s and  $L$ s is tending to the silver ratio as before). This re-ordering fails to fulfill the criteria of Section 3.4, however.

Classes 1, 2b, 3b, 4b, and 4d are inadmissible in any combination, as the rules violate parity. Considering all possible cyclic permutations of the letters within  $\rho$  and  $\lambda$  in the remaining classes, ten can be re-arranged into admissible forms. However, a quick check of the inflated words shows that nine do not constitute quasicrystals. The result is that there is only one additional quasicrystal which can lead to stable attractive orbits in nonlinear dynamical systems. It is defined by the inflation rules of class 3a, adjusted to the following form:

$$R \rightarrow RLR^2, \quad L \rightarrow LR^2 \tag{6}$$

which lead to the substitutions

$$\begin{aligned} R &\rightarrow RLR^2 \\ &\rightarrow RLR^2LR^3LR^3LR^2 \\ &\rightarrow RLR^2LR^3LR^3LR^2LR^3LR^3LR^3LR^2LR^3LR^3LR^3 \dots \end{aligned}$$

*i.e.* words of length 1, 4, 15, 56, 209, ... (OEIS A001353). Up to sign differences these are known as the ‘Clapeyron numbers’ (OEIS A125905) after appearing in a treatise on beam bending by Clapeyron [52]. We name the corresponding words the Clapeyron words  $C_n$ , with the infinite Clapeyron word  $C_\infty$  being the Clapeyron quasicrystal. The ratios of cell lengths of the Clapeyron words asymptotically approach the value

$$2 + \sqrt{3} = \lim_{n \rightarrow \infty} \frac{C_n}{C_{n-1}}.$$

The analyses presented throughout this paper apply equally well to the Clapeyron quasicrystal as to the Pell quasicrystal, although we focus on the simpler Pell case.

## 4.2 Proof of Maximality of the Pell Words

To prove all Pell words are maximal, it is sufficient to show that the Pell substitution rules of Equation (5) obey the generalized composition rules of Section 3.4. We restate and address criteria (1)-(5) of Section 3.4 individually.

(1)  $P(\lambda) = -1, P(\rho) = 1$ :

$$\begin{aligned} P(\rho) &= -P(R)P(L) = 1 \checkmark \\ P(\lambda) &= -P(R)P(RL) = P(R)P(R)P(L) = -1 \checkmark \end{aligned}$$

(2)  $\rho > \lambda$ :

The common word appearing as a leftmost string between  $\rho$  and  $\lambda$  is  $W^* = R$ , which is of odd parity. The next letter in  $\rho$  is  $L$ , and that in  $\lambda$  is  $R$ . Since  $L < R$ , and the common word is of odd parity, this implies that  $\rho > \lambda \checkmark$

(3)  $\rho|_C$  is maximal:

We must check that all finite shifts of the word  $\Sigma = \rho|_C$ , *i.e.* truncations of the word from the leftmost letter, are smaller than  $\Sigma$  itself. The only shifted word is  $\Sigma_1$ :

$$\begin{aligned} \Sigma &= \rho|_C = RC \\ \Sigma_1 &= C. \end{aligned}$$

The common word  $W^* = \text{blank}$ , which contains an even number of  $R$ s (zero) and is therefore even. The next letter  $R > C \therefore \Sigma > \Sigma_1$ , so  $\rho|_C$  is maximal  $\checkmark$

(4)  $\rho\lambda|_C$  is maximal:

$$\Sigma = \rho\lambda|_C = RLRRC$$

and, as before, we check all shifts of the word ( $b$  is the blank word):

$$\begin{aligned} \Sigma_1 &= LRRRC, W^* = b, \text{ even}, L < C \therefore \Sigma > \Sigma_1 \\ \Sigma_2 &= RRRRC, W^* = R, \text{ odd}, L < R \therefore \Sigma > \Sigma_2 \\ \Sigma_3 &= RRC, W^* = R, \text{ odd}, L < C \therefore \Sigma > \Sigma_3 \\ \Sigma_4 &= C, W^* = b, \text{ even}, R > C \therefore \Sigma > \Sigma_4 \end{aligned}$$

$$\therefore S^k(\rho\lambda|_C) < \rho\lambda|_C \quad \forall k$$

and  $\rho\lambda|_C$  is maximal  $\checkmark$

(5)  $\rho\lambda^\infty$  is maximal:

$$\Sigma = \rho\lambda^\infty = RL(RRL)^\infty$$

$$\begin{aligned} \Sigma_1 &= L(RRL)^\infty, W^* = b, \text{ even}, R > L \therefore \Sigma > \Sigma_1 \\ \Sigma_2 &= RRL(RRL)^\infty, W^* = R, \text{ odd}, L < R \therefore \Sigma > \Sigma_2 \\ \Sigma_3 &= RL(RRL)^\infty = \Sigma \end{aligned}$$

therefore

$$S^k(\rho\lambda^\infty) \leq \rho\lambda^\infty \quad \forall k$$

and  $\rho\lambda^\infty$  is maximal  $\checkmark$

The Pell inflation rules therefore obey the generalized composition criteria. Since the word  $R$  is maximal, and the Pell words are generated by application of the Pell inflation rules to  $R$ , all Pell words are therefore maximal, including the Pell quasicrystal  $P_\infty$ .  $\square$

An identical analysis can be applied to the Clapeyron word inflation rules to prove their admissibility, and can be applied to all other quasicrystals listed in Table 1 to see that these two are the only possible time quasicrystals. In all cases the results can be verified by attempting to locate the corresponding values of  $\mu$  using word-lifting: if the words are inadmissible, even a single iteration of  $\mu_{n+1}(\mu_n)$  is likely to fail, whereas the value of  $\mu$  converges for a wide range seed values even for the length 70 Pell word (requiring 69 nested square-root functions).

### 4.3 The Pell Cascade

The transition to chaos in the logistic map comes about through an infinite number of applications of the period-doubling substitutions  $R \rightarrow RL$ ,  $L \rightarrow RR$  applied to the symbol  $R$ . This is known as a period-doubling cascade, as each iteration leads to a word twice the length of its predecessor. The Pell quasicrystal is generated through an infinite number of applications of the Pell inflation rules, Equation 5, to the symbol  $R$ , and we term the sequence the Pell cascade. Just as in the period-doubling cascade, successive terms in the Pell cascade are reached through increasing the value of the parameter  $\mu$  in the logistic map of Equation (2). The first few values, and the limit  $P_\infty$ , are indicated in Figure 4.

The values of the parameter  $\mu$  used to generate successive Pell words as stable attracting orbits in the logistic map are given in Table 2, found using the word lifting technique. In order to give a faster convergence of the numerical iterations, the final letter of each word has been substituted with the central point  $C$ , which makes the corresponding orbit superstable. The word itself can be found by infinitesimally increasing or decreasing  $\mu$  so as to undo this substitution (by appeal to the periodic window theorem). The values of  $\mu$  are converging on a value of  $\mu_\infty = 1.6703\dots$ . This rapid convergence is a consequence of the fact that the Pell numbers  $P_n$  grow faster than  $2^n$ , which itself follows from the additional letter in the symbol  $L$  Pell substitution compared to the period-doubling substitution. The Clapeyron cascade accelerates more rapidly still. While the widths of the periodic windows are rapidly decreasing, in general the window widths are known to be system-dependent, and in any case cannot be said to simply decrease with increasing word length [30, 31].

Note that the successive Pell words do not appear contiguously, as do the successive words in the period-doubling cascade. Periodic windows in a chaotic regime are entered via the intermittency route to chaos, and exited through a period doubling cascade. All the words within one window therefore take the form of a word with the period doubling substitution rules applied to it. It follows that each Pell word longer than  $RL$  appears within its own periodic window in the chaotic regime, and the sequence cannot be contiguous. As a result, although the values of  $\mu$  required to generate each successive word increase monotonically, there may exist additional admissible words between each iteration which are not Pell words. It is possible to find all admissible words between two words by appeal to the periodic window theorem [31]. We omit the details here, but note that even within the chaotic regime, there are still non-Pell words interspersed between the Pell words. For example,

$$P_3 \prec RLR^2LRLC \prec P_4 \prec P_4RLR^2LRLC \prec P_4RLR^2LRC \prec P_5 \prec \dots$$

where ' $A \prec B$ ' indicates that word  $A$  appears at a lower  $\mu$  than word  $B$  in the logistic map.

$P_n$	$\mu_C$	$\mu_-$	$\mu_+$
1	0	0	3/4
2	1	3/4	5/4
5	1.625413725123	1.62443	1.62838
12	1.66964217697186	1.66964	1.66965
29	1.67028686872861	$\mu_C - 3 \times 10^{-10}$	$\mu_C + 2 \times 10^{-9}$
70	1.67028763874509	-	-
$\infty$	$\approx 1.670288$		

Table 2: The sequence of parameters  $\mu_C$  required to give successive superstabilized Pell words  $P_n|_C$ , of length  $P_n$ , as superstable attractive orbits in the logistic map of Equation (2). The first two values are known analytically. The others are found via word lifting, and are accurate to at least the number of digits stated. The lower and upper bound of each periodic window,  $\mu_{\pm}$ , is also stated; the period-70 window is smaller than machine precision ( $10^{-16}$ ).

The inflation property of quasicrystals is key in the present study. Each unit cell  $R$  and  $L$  corresponds to a single iteration of discrete time in the dynamical system, and so these cells are of the same length. A single inflation leads to the cells  $RL$  and  $RRL$ . These are also perfectly good unit cells which can be used to tile the Pell quasicrystal, but are now of different lengths, two and three. This already suffices to define the infinite Pell word, appearing as a stable attracting orbit in discrete-time dynamical systems, as a time quasicrystal: a tiling of the time axis by unit cells of two different durations, forming an aperiodic sequence generated as a slice through a periodic tiling of two-dimensional time. Should it be desired that the durations of the cells, in addition to their frequency of appearance, also lie in the silver ratio, systematic approximations can be formed by repeated action of the inflation rules.

In Figure 5 we show the sequence of points  $x_n$  visited in the first 30 iterations of the logistic map with  $\mu = 1.625\dots$  chosen to give the superstabilized period-5 Pell word  $P_3|_C$ . In Figure 6 we show the temporal Fourier transform of the first 3000 iterations for Pell words  $P_4|_C$ ,  $P_5|_C$ , and  $P_6|_C$  of periods 12, 29, and 70, respectively. The plots demonstrate two important points. First, the largest Bragg peaks in the transforms shift only slightly between successive words. They are converging on their locations in the infinite Pell word, showing that the successive finite words indeed form a systematic approximation to the quasicrystal. The largest Bragg peak is converging on  $(1 + \sqrt{2})^{-1}$ , as expected for the infinite Pell word which is described by two cells with lengths related through the silver ratio  $1 + \sqrt{2}$ . Second, the longer words begin to develop a dense background in addition to the Bragg peaks. This is expected for quasicrystals, which lie between periodicity, which would show sharp Bragg peaks, and disorder, which would show a dense, uniform distribution.

#### 4.4 Other Time Quasicrystals

Other than the infinite Pell and Clapeyron words, no other quasicrystals can possibly be grown as stable attractive sequences in dynamical systems, as the other cases fail to fulfill the generalized composition rules.

It could always be the case that the infinite words describing the other eight quasicrystal classes happen to be stable. For example, the eight-letter Fibonacci word  $RLRRLRLR$  happens to be stable despite the Fibonacci inflation rules not fitting the composition criteria.

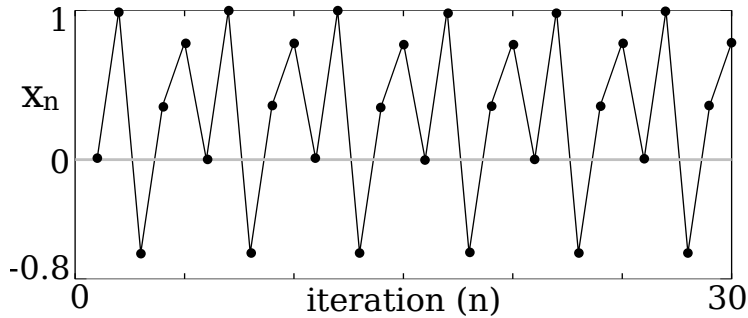


Figure 5: The sequence of points  $x_n$  visited in the logistic map with  $\mu = 1.625\dots$  chosen to give the superstabilized period-5 Pell word  $P_3$ .

Other examples exist, and we cannot rule out the possibility that the Fibonacci quasicrystal is also stable. Without a systematic growth rule it is not clear how this could be seen. Even if the infinite word could be shown to be stable but lacking in a systematic growth mechanism, the result would not be testable in any finite-duration experiment, so would be physically uninteresting.

Nevertheless, taking again the example of the infinite Fibonacci word, searching along its length we can find many sub-words of any desired finite length. If we find a sub-word which is admissible as a stable periodic orbit, it could still be used as a periodic approximation to the Fibonacci quasicrystal. In effect, we would simply be starting the Fibonacci word at a different point in time. To construct a set containing all the possible sub-words (and more) we note that the Fibonacci inflation rules imply that neither two  $L$ s nor three  $R$ s are ever adjacent in the word. We could then consider all possible words of a given length consisting of the letters  $L$  and  $R$  and excluding words according to this observation. Actually, an infinite hierarchy of such restrictions is necessary: it is also true that neither two blocks of  $RL$  nor three blocks of  $RLR$  are ever adjacent, for instance. Such systems are considered elsewhere, for example in references [26, 53], where they are treated by various techniques of combinatorics.

Sub-words of the infinite Fibonacci word can be found which describe stable admissible orbits of most lengths. The number of distinct  $n$ -letter sub-words of the Fibonacci quasicrystal is  $n + 1$ . Searching all possible sub-words up to length 500, the cumulative total number of admissible words appears to grow as a logarithmic Devil's staircase, as shown in Fig. 7. However, even in the instances of admissible sub-words, we re-iterate that without a systematic growth mechanism such as we have found for the Pell and Clapeyron quasicrystals, the result is uninteresting from a physical point of view.

## 5 Pell Words in Continuous-Time Dynamical Systems

The work so far has focussed on the logistic map of Eq. (2), a discrete-time dissipative dynamical system [34]. In this section we generalize our results to a range of continuous-time dynamical systems, in order to provide physically testable examples.

We proceed as follows. In Section 5.1 we consider a continuous-time dissipative system without driving, the Rössler attractor, and show that the results obtained for the logistic map extend to this system. Lacking predefined time steps, however, the duration of each

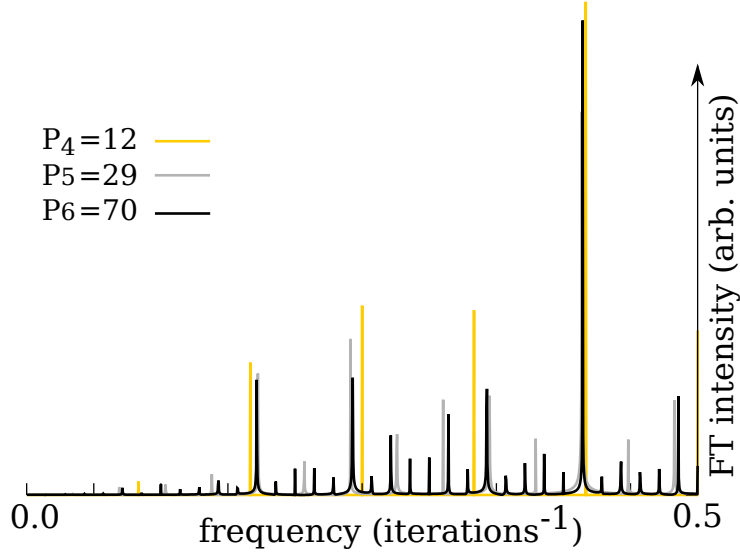


Figure 6: Temporal Fourier transforms of the sequences of points visited for superstable Pell words  $P_4$ ,  $P_5$ ,  $P_6$  (periods 12, 29, 70). 3000 points are taken in each run. The Bragg peaks are converging on the quasicrystal values, demonstrating that the successive Pell words constitute a systematic approximation scheme to the infinite word, while a dense background begins to form demonstrating the quasicrystalline nature of the infinite word.

step ceases to be stable to perturbations, and the result is no longer a time quasicrystal in the desired sense. In Section 5.2 we consider a continuous-time periodically-driven dissipative system, the forced Brusselator, in which the length of each period of the time quasicrystal is fixed by the periodicity of the external driving. This constitutes a time quasicrystal in a continuous-time dissipative system. In both cases the systems considered are specific cases used to illustrate much wider classes.

### 5.1 A Continuous-Time Dissipative Autonomous System: the Rössler Attractor

The Rössler system is defined by the continuous-time equations of motion:

$$\begin{aligned}\dot{x}(t) &= -y - z \\ \dot{y}(t) &= x + ay \\ \dot{z}(t) &= b + z(x - c).\end{aligned}\tag{7}$$

The system is dissipative. For a wide range of parameters the system features a strange attractor. The case of  $a = 0.2$ ,  $b = 0.5$ ,  $c = 5.7$  is shown in Fig. 8. We define a Poincaré section through the attractor by finding its intersections with the half-plane  $x = 0$ ,  $y > 0$ . The trajectories' intersections with the plane are shown in the figure.

We use the Poincaré section to construct a Poincaré first return map, plotting the  $y$  coordinate at intersection  $n + 1$ ,  $y_{n+1}$ , against the  $y$  co-ordinate of the previous intersection  $y_n$ . The map is unimodal, bearing a strong resemblance to the logistic map. The first return map is shown for three values of the parameter  $b$  in Fig. 9. Note that the maps are well-

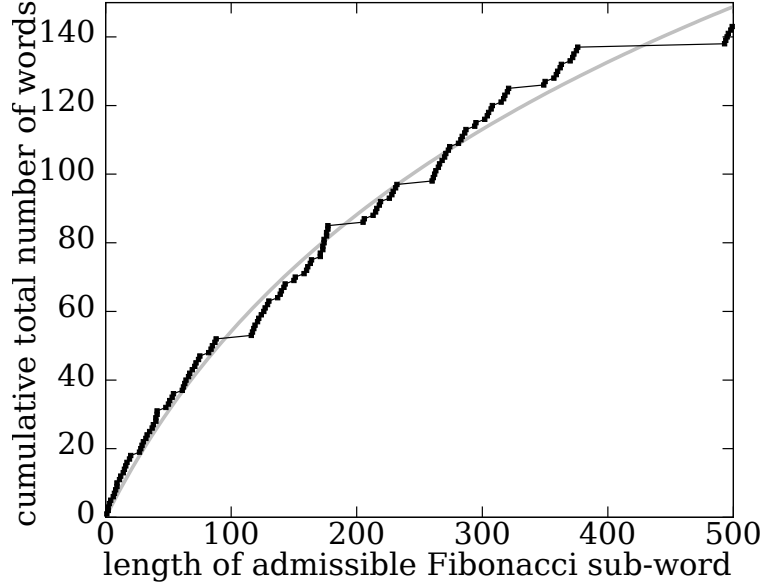


Figure 7: Black points: the cumulative total number of admissible words (in the sense of the universal sequence) found in the sub-words of the Fibonacci quasicrystal up to a given length. Black lines connect the points. Silver curve: logarithmic fit to the data,  $y = 93.1 \log(1 + x/126.6)$ . There are  $n + 1$  sub-words of the Fibonacci quasicrystal of length  $n$ , so the cumulative total number of sub-words up to length  $n$ , neglecting admissibility, is  $\frac{1}{2}(n + 1)(n + 2)$ .

approximated by 1D lines, which follows from the large dissipation in the Rössler equations of motion.

Varying  $b$  over the range  $0 < b < 2$  we find all the qualitative features derived for the logistic map. In Figure 10 we plot an orbit diagram for the Rössler system by plotting  $y_{5000}$  to  $y_{8000}$  (it is assumed stable orbits have been reached after this many iterations) against  $2 - b$ . Chaos develops via a period-doubling cascade reached by around  $2 - b = 1.3$ . The universal sequence of periodic windows within the chaotic regime is again visible, with the period-6 orbit just below  $2 - b = 1.4$ , and the period-3 orbit at around  $2 - b = 1.65$ . The maxima in the first-return maps vary as a function of  $b$ , and we have located and plotted them on the orbit diagram in black. These constitute the superstable points in the orbits. Note that each periodic window again has a superstable point contained within it.

As an example of a Pell word in the Rössler system, the period-5 window can be seen around  $2 - b \approx 1.5$ . Zooming in, we found the window to be located around  $2 - b \approx 1.492$ . Setting this parameter value, the system rapidly converges to a period-5 orbit, which has intersections with the first return map described by the word  $RLRRC$ . A slight decrease of  $2 - b$  then stabilizes the Pell word  $P_5 = RLRRL$ . The  $2 - b = 1.492$  first-return map (after allowing transients to die down) is shown superposed on the close-by  $2 - b = 1.5$  chaotic map in Figure 11, along with the cobweb which generates it in the discrete-time 1D map. Figure 12 shows the trajectory itself.

The results match nicely with those predicted by the logistic map. From the existence of the universal sequence in the Rössler system it follows that the Pell words, including the



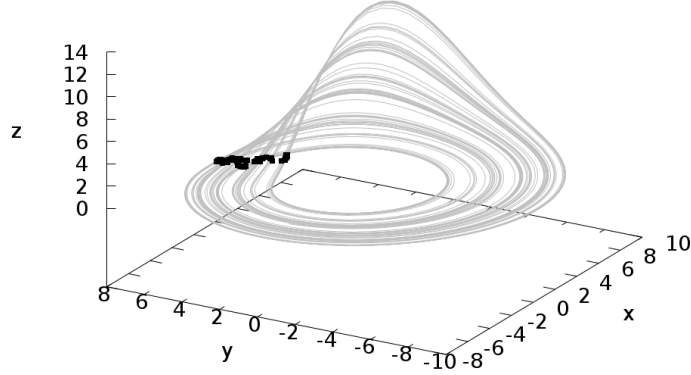


Figure 8: The Rössler strange attractor given by Eq. (7) for parameter values  $a = 0.2$ ,  $b = 0.5$ ,  $c = 5.7$ . The black points mark the intersections with the Poincaré section given by the half-plane  $x = 0$ ,  $y > 0$ . We iterated the equations of motion, Equation (7), using a fourth-order Runge-Kutta algorithm.

infinite Pell word, exist as stable attracting orbits in the Poincaré first-return map. A qualitatively similar, physically-implemented system is the Belousov-Zhabotinsky autocatalytic chemical reaction [54–56]. This system, too, is known to feature the universal sequence, and therefore also features the Pell words as admissible trajectories.

However, having moved to continuous time, neither system can reasonably be described as a time quasicrystal. Although the sequence of  $L$ s and  $R$ s visited by the trajectory remains fixed, the ‘time of flight’ between successive intersections of the Poincaré section is neither fixed, nor stable to perturbation. In order to find such stability, we consider a periodically driven dissipative system in the next section.

## 5.2 A Continuous-Time Dissipative Driven System: the Forced Brusselator

The forced Brusselator (portmanteau of ‘Brussels’ and ‘oscillator’) is described by the equations

$$\begin{aligned}\dot{x}(t) &= A - (B + 1)x + x^2y + \alpha \cos(\omega t) \\ \dot{y}(t) &= Bx - x^2y.\end{aligned}\tag{8}$$

The undriven model with  $\alpha = 0$  has been used to model certain autocatalytic chemical reactions, and again bears similarity to the Belousov-Zhabotinsky reaction [55–57]. Featuring an external driving frequency  $\omega$  the equations are non-autonomous, although they can be rewritten as an autonomous set of four equations by defining

$$\begin{aligned}u(t) &= \cos(\omega t) \\ \dot{u}(t) &= -\omega u \\ \dot{z}(t) &= \omega u\end{aligned}$$

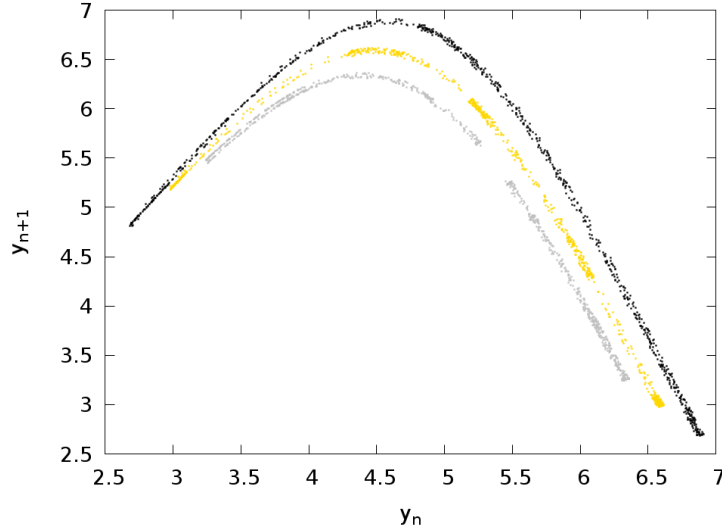


Figure 9: The Poincaré first-return map obtained from the Rössler equations of motion (*cf.* Fig. 8) by plotting the  $y$  co-ordinate,  $y_{n+1}$ , of intersection  $n + 1$  with the Poincaré section  $x = 0$ ,  $y > 0$ , against the  $y$  co-ordinate of the previous intersection  $y_n$ . The parameters are  $a = 0.2$ ,  $c = 5.7$ ,  $2 - b = 1.4$  (silver),  $2 - b = 1.5$  (gold),  $2 - b = 1.6$  (black). Note that the maxima shift slightly as a function of the varying parameter  $b$ .

which can then be iterated using a Runge-Kutta algorithm. The natural Poincaré section to take is now any constant  $u$  plane, corresponding to a periodic sampling of the system. Note that admission to the section is dependent upon the trajectory crossing with the correct orientation.

The phase space of the equations is quite complex. While it does feature period-doubling cascades as functions of various parameters, we were unable to locate any leading directly into universal sequences as in the previous examples. Nevertheless, the existence of the universal sequence words within the system has previously been confirmed [31, 57].

Taking the parameter values  $A = 0.38$ ,  $B = 1.2$ ,  $\alpha = 0.05$ , we find that a chaotic regime at frequency  $\omega = 0.72$  develops into a stable period-5 window at  $\omega = 0.725$ . In Figure 13 we show the Poincaré first-return map obtained from the Poincaré section  $u = 0$  crossed in a positive sense, for both the chaotic response (gold) and period-5 response (black). As before, we see that the trajectory is described by the Pell word  $RLRRL$  (this frequency is slightly away from the superstable point  $RLRRC$ , so the word itself appears). In Figure 14 we show the period-5 trajectory and the Poincaré section.

The forced Brusselator system has the advantage over the Rössler system that the time taken between intersections of the Poincaré section is fixed to be a multiple of the driving frequency. The cell lengths  $R$  and  $L$  are therefore identically equal to one period of the driving, and are stable to perturbations either of other system parameters or to random kicks to the trajectory. Subsequent inflations such as  $RL$ ,  $RRL$  constitute two different cell lengths which can be used to tile longer Pell words when located in the system, including (in principle) the Pell quasicrystal.

It should be noted that the forced Brusselator does not fall into the same universality class as the Rössler system or the logistic map, as it features a cubic nonlinearity. Fortunately,

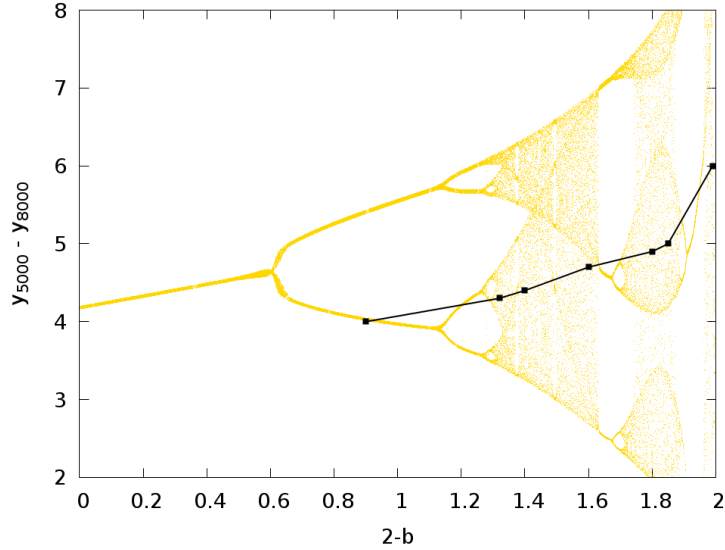


Figure 10: Orbit diagram for the Rössler system found by plotting intersections  $y_{5000}$  to  $y_{8000}$  of the Poincaré section for a range of parameters  $b$ . It is assumed stable orbits have been converged to for parameters at which they exist. The maxima of the first-return maps have been used to identify the superstable line shown in black (points indicate identified maxima). All qualitative features of the logistic map appear, including a period-doubling cascade into chaos, and a series of periodic windows following the universal sequence which have opened around superstable orbits.

this is not necessary for the words of the universal sequence to appear as stable orbits on the associated Poincaré map. In fact, the universal sequence has previously been identified in the forced Brusselator system [31]. This is important: if we know that the universal sequence appears, even in a re-ordered form, it means that all Pell and Clapeyron words appear. This means we can make periodic approximations to the Pell and Clapeyron quasicrystals of arbitrary duration, by refining our experimental precision. If the universal sequence does not appear, it may be that individual words can be found regardless, but the process may fail at or above a given duration. Furthermore, without some reason to believe that all the words appear in principle, we are merely investigating periodic orbits of the first-return maps, as opposed to using them as periodic approximations to time quasicrystals.

The forced Brusselator is stabilized to perturbations in part by its dissipation (the equations of motion can again not be rewritten into a Hamiltonian form). Despite lacking a conserved quantity which can be thought of as energy, it is still possible to define a temperature-like external noise in dissipative systems, at least away from the superstable points. Robustness of the trajectories to finite temperature can be established through a renormalization group analysis [31]. Further work is required before it could be claimed that such a system also constitutes a ‘state of matter’, as was shown in the experimental implementation of time crystals [11, 12].

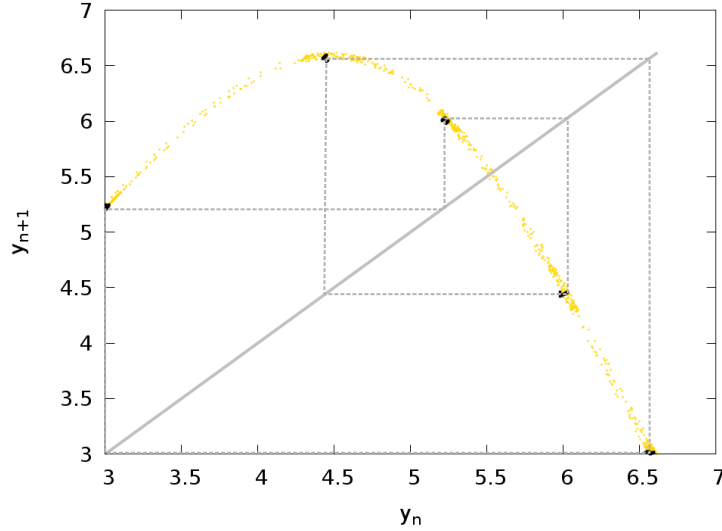


Figure 11: In gold is a reproduction of the  $2 - b = 1.5$  first-return map from Fig. 9. In black is the first-return map for  $2 - b = 1.492$ . The slight change in parameter takes us into a period-5 window stabilized by the superstable orbit described by the superstabilized Pell word  $P_5|_C = RLLRC$  (the first 5000 steps have been omitted so that the periodic orbit is reached). The cobweb has been added to emphasize how the results for discrete-time maps have carried to this continuous-time system.

## 6 Conclusion

In this paper we have demonstrated the existence of time quasicrystals in dissipative dynamical systems. These are aperiodic tilings of the time axis with two different unit cells, which can be constructed as slices through two orthogonal time directions. We demonstrated that time quasicrystals can appear as stable, attracting orbits in any dissipative nonlinear dynamical system which features the universal sequence, or any re-ordering thereof [31,36]. This is a wide universality class, encompassing physical applications in the study of animal populations [35], chemical reactions [55,56], hydrodynamics [58], and electronics [59,60], to name a few. We demonstrated that these time quasicrystals can be ‘grown’ by repeated application of their inflation rules, meaning that systematic finite periodic approximations can be found in any system in which they exist, giving an experimentally-testable method of searching for them.

Of the ten equivalence classes of physically-relevant one-dimensional quasicrystals recently identified by Boyle and Steinhardt [25], we find that precisely two are able to form time quasicrystals. These are class 2a, the infinite Pell word  $P_\infty$  related to the silver ratio  $1 + \sqrt{2}$ , and class 3a, the infinite Clapeyron word  $C_\infty$  related to  $2 + \sqrt{3}$ . The relevance of these cases is that they generalize to higher-dimensional quasicrystals which can be grown in the lab [21,22]. Class 2 generalizes to the Ammann-Beenker tiling, a two-dimensional tiling with an 8-fold rotationally-symmetric diffraction pattern, and class 3 generalizes to the cases of two-dimensional tilings with 12-fold rotationally-symmetric diffraction patterns [20].

It is necessary to consider the time quasicrystals’ place in the set of periodic space-time orders discussed in the Introduction. Choreographic crystals constitute an extension of the

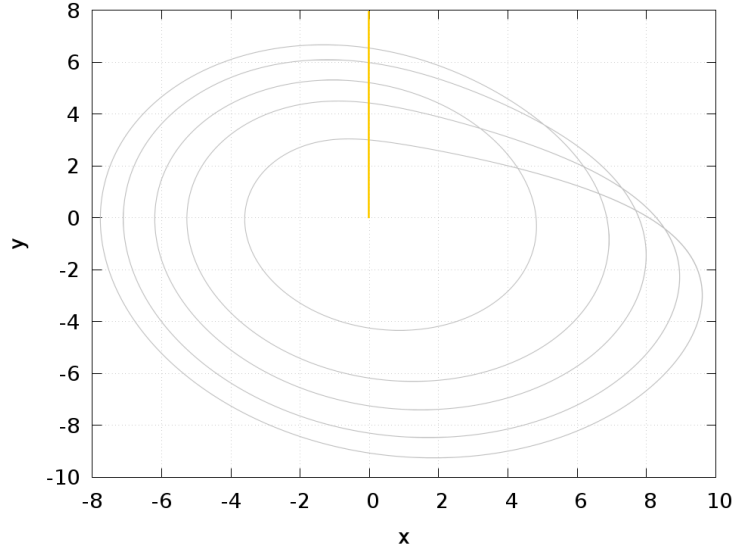


Figure 12: The projection into the  $xy$  plane of the continuous-time orbit generated by the superstabilized Pell word  $P_5|_C = RLLRC$ , found by setting  $a = 0.2$ ,  $2 - b = 1.492$ ,  $c = 5.7$  in the Rössler equations and iterating for 5000 steps before plotting so as to allow the orbit to stabilize. In gold is the Poincaré section.

concept of space group symmetry to encompass the time direction [13]. The interesting cases contain multiple moving elements, whereas the time quasicrystals discussed here focus on the trajectory of a single particle. Interestingly, chaotic systems can demonstrate synchronization when coupled, while maintaining their unpredictability [29, 45, 61]. This synchronization can take the form of a fixed delay between points on the particles' trajectories. Since both periodicity and chaos can synchronize it would seem likely that time quasicrystals, lying between the two, can do so as well. This would suggest a multi-particle implementation of dissipative time quasicrystals which could feature an enhanced choreographic order.

Discrete time crystals spontaneously break the discrete time translation symmetry of a periodic driving force with a response of twice the period [7–10]. They are also required to be stabilized to finite temperature through the interactions of many degrees of freedom, fitting our intuition for what constitutes a ‘state of matter’. There should also be some sense in which they can be considered the ground state of a system, as with crystals in space. The following steps would need to be taken before time quasicrystals meet these criteria. A Hamiltonian system would need to be located with a sufficiently one-dimensional Poincaré first-return map, which demonstrates the universal sequence of admissible words. The system would either need to be constructed from a macroscopic number of degrees of freedom, or a macroscopic number of such systems would need to be coupled, such that the interactions between the degrees of freedom stabilize the order to finite temperature. We note that dissipation is not the key criterion for the existence of an effective one-dimensional Poincaré first-return map: hyperbolicity is [26, 53]. This requires that the flow have at least one positive, one negative, and one zero Lyapunov exponent, with the associated eigenvectors giving the directions of the unstable, stable, and marginal manifolds of the flow [40, 41]. The proof of such a property has not even been rigorously established for the Rössler map, but numerical evidence for it exists in a wide range of systems, including Hamiltonian [30, 45, 53]. The universal sequence,

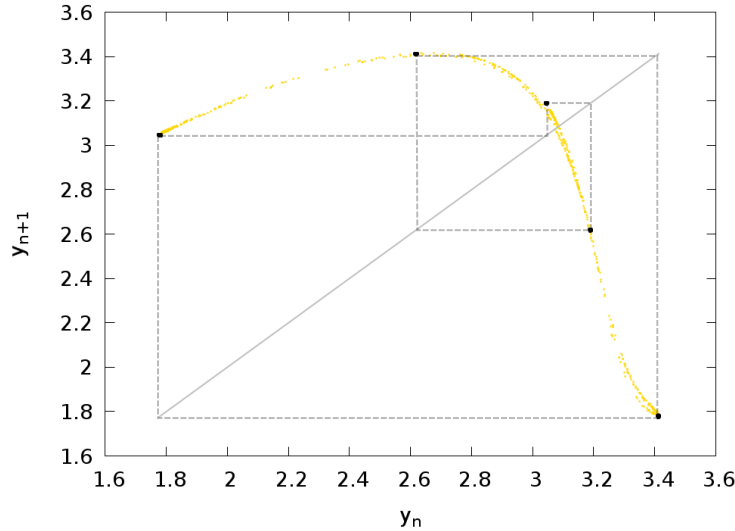


Figure 13: The Poincaré first-return map obtained from Poincaré section  $u = 0$  of the forced Brusselator of Equation (8) with  $A = 0.38$ ,  $B = 1.2$ ,  $\alpha = 0.05$ . In gold are the points obtained at driving frequency  $\omega = 0.72$ , where the response is chaotic. In black are the points obtained at driving  $\omega = 0.725$  which gives a stable period-5 orbit described by the Pell word  $RLRRL$ . The equations were iterated with a fourth-order Runge-Kutta algorithm iterated  $10^5$  steps, discarding the first 5000 steps to allow transients to decay.

as its name suggests, is ubiquitous. Together, these facts suggest it may be quite plausible to bring time quasicrystals in line with the criteria of time crystals. After a pre-print of this paper appeared online, a related pre-print appeared providing a proposal for two physical implementations of dissipative many-body time crystals, fulfilling these criteria [62]. The work identifies a period-doubling cascade, and therefore provides a physical implementation of the results presented here leading to a dissipative many-body time quasicrystal.

From a theoretical perspective, perhaps the most exciting application of time quasicrystals could be as a test of theories concerning multiple dimensions of time. Higher dimensions of space are routinely discussed in the theoretical physics literature, and quasicrystals have been proposed as implementations in several recent papers [63–67]. Higher time dimensions are occasionally considered, but have received relatively less attention [68–70]. It is our hope that the present suggestion of the possibility of testing such theories will lead to wider discussion of such ideas.

## Acknowledgements

The author wishes to thank M. V. Berry, J. P. Keating, M. A. Porter, J. van Wezel, N. Y. Yao, and M. Zaletel for many helpful discussions, and L. Boyle for both helpful discussions and a critical reading of the manuscript.

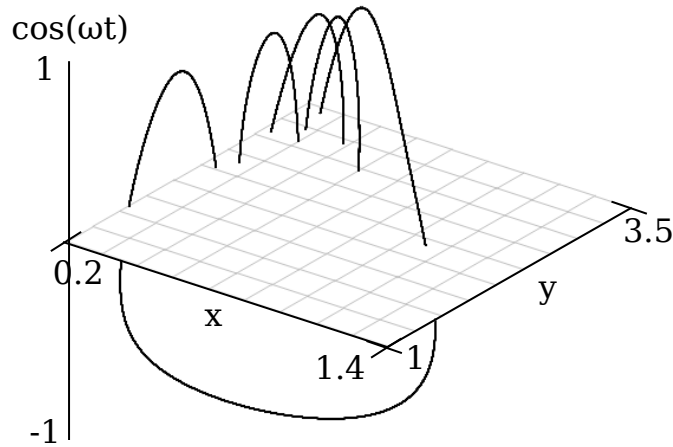


Figure 14: The trajectory followed by the forced Brusselator equations of motion in the period-5 window considered in Figure 13. The Poincaré section  $u = \cos(\omega t)$  is shown (only trajectories passing from negative to positive  $u$  are included).

**Funding information** The author acknowledges support from a Lindemann Trust Fellowship of the English-Speaking Union and the Astor Junior Research Fellowship of New College, Oxford.

## References

- [1] F. Wilczek, *Quantum time crystals*, Phys. Rev. Lett. **109**, 160401 (2012), doi:10.1103/PhysRevLett.109.160401.
- [2] A. Shapere and F. Wilczek, *Classical time crystals*, Phys. Rev. Lett. **109**, 160402 (2012), doi:10.1103/PhysRevLett.109.160402.
- [3] T. Li, Z.-X. Gong, Z.-Q. Yin, H. T. Quan, X. Yin, P. Zhang, L.-M. Duan and X. Zhang, *Space-time crystals of trapped ions*, Phys. Rev. Lett. **109**, 163001 (2012), doi:10.1103/PhysRevLett.109.163001.
- [4] P. Bruno, *Comment on “quantum time crystals”*, Phys. Rev. Lett. **110**, 118901 (2013), doi:10.1103/PhysRevLett.110.118901.
- [5] P. Bruno, *Comment on “space-time crystals of trapped ions”*, Phys. Rev. Lett. **111**, 029301 (2013), doi:10.1103/PhysRevLett.111.029301.
- [6] H. Watanabe and M. Oshikawa, *Absence of quantum time crystals*, Phys. Rev. Lett. **114**, 251603 (2015), doi:10.1103/PhysRevLett.114.251603.
- [7] K. Sacha, *Modeling spontaneous breaking of time-translation symmetry*, Phys. Rev. A **91**, 033617 (2015), doi:10.1103/PhysRevA.91.033617.

- [8] N. Y. Yao, A. C. Potter, I.-D. Potirniche and A. Vishwanath, *Discrete time crystals: Rigidity, criticality, and realizations*, Phys. Rev. Lett. **118**, 030401 (2017), doi:10.1103/PhysRevLett.118.030401.
- [9] D. V. Else, B. Bauer and C. Nayak, *Floquet time crystals*, Phys. Rev. Lett. **117**, 090402 (2016), doi:10.1103/PhysRevLett.117.090402.
- [10] V. Khemani, A. Lazarides, R. Moessner and S. L. Sondhi, *Phase structure of driven quantum systems*, Phys. Rev. Lett. **116**, 250401 (2016), doi:10.1103/PhysRevLett.116.250401.
- [11] J. Zhang, P. W. Hess, A. Kyprianidis, P. Becker, A. Lee, J. Smith, G. Pagano, I.-D. Potirniche, A. C. Potter, A. Vishwanath, N. Y. Yao and C. Monroe, Nature **543**, 217 (2017).
- [12] S. Choi, J. Choi, R. Landig, G. Kucsko, H. Zhou, J. Isoya, F. Jelezko, S. Onoda, H. Sumiya, V. Khemani, C. von Keyserlingk, N. Y. Yao *et al.*, Nature **543**, 221 (2017).
- [13] L. Boyle, J. Y. Khoo and K. Smith, *Symmetric satellite swarms and choreographic crystals*, Phys. Rev. Lett. **116**, 015503 (2016), doi:10.1103/PhysRevLett.116.015503.
- [14] T. Morimoto, H. C. Po and A. Vishwanath, *Floquet topological phases protected by time glide symmetry*, Phys. Rev. B **95**, 195155 (2017), doi:10.1103/PhysRevB.95.195155.
- [15] J. E. S. Socolar and P. J. Steinhardt, *Quasicrystals. ii. unit-cell configurations*, Phys. Rev. B **34**, 617 (1986), doi:10.1103/PhysRevB.34.617.
- [16] C. Janot, *Quasicrystals: A Primer*, Oxford University Press (1994).
- [17] M. Senechal, *Quasicrystals and Geometry*, Cambridge University Press (1995).
- [18] M. Baake and U. Grimm, *Aperiodic Order Volume 1: A Mathematical Invitation*, Cambridge University Press (2014).
- [19] L. S. Levitov, *Why only quadratic irrationalities are observed in quasi-crystals?*, Europhys. Lett. **6**, 517 (1988).
- [20] J. E. S. Socolar, *Simple octagonal and dodecagonal quasicrystals*, Phys. Rev. B **39**, 10519 (1989), doi:10.1103/PhysRevB.39.10519.
- [21] N. Wang, H. Chen and K. H. Kuo, *Two-dimensional quasicrystal with eightfold rotational symmetry*, Phys. Rev. Lett. **59**, 1010 (1987), doi:10.1103/PhysRevLett.59.1010.
- [22] T. Ishimasa, H.-U. Nissen and Y. Fukano, *New ordered state between crystalline and amorphous in ni-cr particles*, Phys. Rev. Lett. **55**, 511 (1985), doi:10.1103/PhysRevLett.55.511.
- [23] L. Bindi, P. J. Steinhardt, N. Yao and P. J. Lu, Science **324**, 1306 (2009).
- [24] L. Bindi, N. Yao, C. Lin, L. S. Hollister, C. L. Andronicos, V. V. Distler, M. P. Eddy, A. Kostin, V. Kryachko, G. J. MacPherson, W. M. Steinhardt, M. Yudovskaya *et al.*, Sci. Rep. **5**, 9111 (2015).



- [25] L. Boyle and P. Steinhardt, *Self-similar one-dimensional quasilattices*, arXiv:1608.08220 [math-ph] (2016).
- [26] R. Badii and A. Politi, *Complexity – Hierarchical Structures and Scaling in Physics*, Cambridge University Press (1997).
- [27] L. Boyle and P. Steinhardt, *Coxeter pairs, ammann patterns and penrose-like tilings*, arXiv:1608.08215 [math-ph] (2016).
- [28] R. Penrose, *The role of aesthetics in pure and applied mathematical research*, Bulletin of the Institute of Mathematics and its Applications **10**, 266ff (1974).
- [29] S. H. Strogatz, *Nonlinear Dynamics and Chaos*, Westview Press, Perseus Books, Cambridge MA (1994).
- [30] K. Alligood, T. D. Sauer and J. A. Yorke, *Chaos: An Introduction to Dynamical Systems*, Springer-Verlag New York (1996).
- [31] B.-L. Hao, *Elementary Symbolic Dynamics and Chaos in Dissipative Systems*, World Scientific, Singapore (1989).
- [32] P. Grassberger, *On symbolic dynamics of one-humped maps of the interval*, Z. Naturforsch. **43a**, 671 (1988).
- [33] S. Isola and A. Politi, *Universal encoding for unimodal maps*, J. Stat. Phys. **61** (1990).
- [34] P. Collet and J.-P. Eckmann, *Iterated Maps on the Interval as Dynamical Systems*, Birkhäuser Berlin (1980).
- [35] R. M. May, Nature **261**, 459 (1976).
- [36] N. Metropolis, M. L. Stein and P. R. Stein, Journal of Combinatorial Theory (A) **15**, 25 (1973).
- [37] O. E. Rössler, *An equation for continuous chaos*, Physics Letters A **57**(5), 397 (1976).
- [38] F. Flicker and J. van Wezel, *One-dimensional quasicrystals from incommensurate charge order*, Phys. Rev. Lett. **115**, 236401 (2015), doi:10.1103/PhysRevLett.115.236401.
- [39] N. P. Fogg, *Substitutions in Dynamics, Combinatorics, and Arithmetic*, Springer-Verlag Berlin (2002).
- [40] D. V. Anosov, *Geodesic flows on closed riemannian manifolds of negative curvature*, Trudy Mat. Inst. Steklov. **90**, 3 (1967).
- [41] S. Smale, Bull. Amer. Math. Soc. **73**, 747 (1967).
- [42] E. Ott, C. Grebogi and J. A. Yorke, *Controlling chaos*, Phys. Rev. Lett. **64**, 1196 (1990), doi:10.1103/PhysRevLett.64.1196.
- [43] T. Shinbrot, C. Grebogi, J. A. Yorke and E. Ott, Nature **363**, 411 (1993).
- [44] K. Pyragas, Physics Letters A **170**, 421 (1992).

- [45] J. M. Gonzalez-Miranda, *Synchronization and Control of Chaos*, Imperial College Press (2004).
- [46] P. T. Dumitrescu, R. Vasseur and A. C. Potter, *Logarithmically slow relaxation in quasi-periodically driven random spin chains*, arXiv:1708.00865 [cond-mat.dis-nn] (2017).
- [47] M. J. Feigenbaum, *The universal metric properties of nonlinear transformations*, J. Stat. Phys. **21**, 669 (1979).
- [48] M. J. Feigenbaum, *The metric universal properties of period doubling bifurcations and the spectrum for a route to turbulence*, Ann. New York. Acad. Sci. **357**, 330 (1980).
- [49] N. J. A. Sloane, *The On-Line Encyclopedia of Integer Sequences*, published electronically at <https://oeis.org> (2017).
- [50] *Lettre IX. Euler à Goldbach, 10 August 1750, in: Correspondance Mathématique et Physique de Quelques Célèbres Géomètres du XVIIIeme Siècle.*
- [51] N. G. de Bruijn, *Sequences of zeros and ones generated by special production rules*, Indagationes Mathematicae (Proceedings) pp. bf 84, 27 (1981).
- [52] B. Clapeyron, *Calcul d'une poutre élastique reposant librement sur des appuis inégalement espacés*, Comptes rendus hebdomadaires des séances de l'Académie des Sciences **45**, 1076 (1857).
- [53] P. Cvitanović, R. Artuso, R. Mainieri, G. Tanner and G. Vattay, *Chaos: Classical and Quantum*, Niels Bohr Institute, Copenhagen, doi:www.chaosbook.org (2016).
- [54] A. M. Zhabotinsky, Chaos **1**, 379 (1991).
- [55] J.-C. Roux, R. H. Simoyi and H. L. Swinney, *Observation of a strange attractor*, Physica D **8**, 257 (1983).
- [56] F. Argoul, A. Arneodo, P. Richetti, J. C. Roux and H. L. Swinney, *Chemical chaos: From hints to confirmation*, Acc. Chem. Res. **20**, 436 (1987).
- [57] B.-L. Hao, G.-R. Wang and S.-Y. Zhang, *U-sequences in the periodically forced brusselator*, Communications in Theoretical Physics **2**(3), 1075 (1983).
- [58] M. Giglio, S. Musazzi and U. Perini, *Transition to chaotic behavior via a reproducible sequence of period-doubling bifurcations*, Phys. Rev. Lett. **47**, 243 (1981), doi:10.1103/PhysRevLett.47.243.
- [59] P. S. Linsay, *Period doubling and chaotic behavior in a driven anharmonic oscillator*, Phys. Rev. Lett. **47**, 1349 (1981), doi:10.1103/PhysRevLett.47.1349.
- [60] J. Testa, J. Pérez and C. Jeffries, *Evidence for universal chaotic behavior of a driven nonlinear oscillator*, Phys. Rev. Lett. **48**, 714 (1982), doi:10.1103/PhysRevLett.48.714.
- [61] A. Arenas, A. Díaz-Guilera, J. Kurths, Y. Moreno and C. Zhou, *Synchronization in complex networks*, Physics Reports **469**(3), 93 (2008), doi:<https://doi.org/10.1016/j.physrep.2008.09.002>.

- [62] Z. Gong, R. Hamazaki and M. Ueda, *Discrete time-crystalline order in cavity and circuit qed systems*, arXiv:1708.01472 [cond-mat.stat-mech] (2017).
- [63] S. Weinberg, *The Quantum Theory of Fields: Volume 3, Supersymmetry*, Cambridge University Press (2000).
- [64] E. Witten, *Search for a realistic kaluza-klein theory*, Nuclear Physics B **186**(3), 412 (1981).
- [65] Y. E. Kraus, Y. Lahini, Z. Ringel, M. Verbin and O. Zilberberg, *Topological states and adiabatic pumping in quasicrystals*, Phys. Rev. Lett. **109**, 106402 (2012), doi:10.1103/PhysRevLett.109.106402.
- [66] Y. E. Kraus, Z. Ringel and O. Zilberberg, *Four-dimensional quantum hall effect in a two-dimensional quasicrystal*, Phys. Rev. Lett. **111**, 226401 (2013), doi:10.1103/PhysRevLett.111.226401.
- [67] K. A. Madsen, E. J. Bergholtz and P. W. Brouwer, *Topological equivalence of crystal and quasicrystal band structures*, Phys. Rev. B **88**, 125118 (2013), doi:10.1103/PhysRevB.88.125118.
- [68] P. A. M. Dirac, *Wave equations in conformal space*, Annals of Mathematics **37**(2), 429 (1936).
- [69] I. Bars, *Gauge symmetry in phase space consequences for physics and spacetime*, International Journal of Modern Physics A **25**(29), 5235 (2010).
- [70] R. Dijkgraaf, B. Heidenreich, P. Jefferson and C. Vafa, *Negative branes, supergroups and the signature of spacetime*, arXiv:1603.05665 [hep-th] (2016).